NEOPLASIA
www.neoplasia.com
Volume 23 Number xxx Month 2021 pp. 36–48

Original Research

Eucannabinolide, a novel sesquiterpene lactone, suppresses the growth, metastasis and BCSCS-like traits of TNBC via inactivation of STAT3☆,☆☆

Zhihui Zhu[1]; Jingtao Yuan[1]; Xintong Xu; Yingying Wei; Bo Yang*; Huajun Zhao*

College of Pharmaceutical Sciences, Zhejiang Chinese Medical University, Hangzhou, Zhejiang, China

Abstract

Signal transducer and activator of transcription 3 (STAT3) is an important therapeutic target to triple negative breast cancer (TNBC) treatment. In the present study, we aim to investigate the potential activity of Eucannabinolide (Euc), a novel sesquiterpene lactone separated from Eupatorium cannabinum Linn. against TNBC by targeting STAT3 and expect that Euc will be developed as an inhibitor of STAT3 in the treatment of TNBC. We found that Euc effectively suppressed STAT3 activation at tyrosine 705, inhibited its translocation to nucleus, and decreased its DNA binding capacity. Moreover, introduction of STAT3-short hairpin RNAs or STAT3 inhibitor S3I-201 attenuates the Euc-induced inhibition of cell viability. And, Euc inhibited cell viability, proliferation, metastasis and breast cancer stem cell-like traits but did not induce cytotoxicity in human mammary epithelial cells. The *in vivo* study similarly demonstrated that administration of Euc inhibited the growth of xenograft tumors and impaired tumor metastasis of a lung metastasis model. The above phenomena were associated with STAT3 dysfunction induced by Euc. In conclusion, Euc elicits the effects of anti-proliferation, anti-metastasis and anti-breast cancer stem cell-like traits in TNBC via targeting STAT3. These data highlight that development of Euc as a STAT3 inhibitor may offer a promising therapeutic strategy for TNBC.

Neoplasia (2021) 23, 36–48

Key words: Eucannabinolide, Triple negative breast cancer, STAT3, Proliferation, Metastasis, Breast cancer stem cells

Introduction

Breast cancer is one of the three most common cancers in the world and has the highest incidence in women [1]. Triple negative breast cancer (TNBC) is one of the five subtypes in breast cancer based on the absence of estrogen receptor, progesterone receptor, and human epidermal growth factor-2, accounts for 10% to 20% of all breast cancer [2]. Currently, targeted therapies (PARP inhibitors and EGFR inhibitors) or immunotherapies are preliminary used in clinic and showing promising effects. However, many TNBC patients remain unresponsive, resulting in poor prognosis [3–5]. Further studies need to be investigated.

Abnormal activation of carcinogenic signal transduction pathway is a key link in the occurrence and development of cancer. The dependence of cancer cells rather than normal cells on this survival pathway is the basis of targeted therapy [6]. Signal transducer and activator of transcription 3 (STAT3) is a cancer-dependent transcription factor, associated with the proliferation, metastasis, angiogenesis and chemo-resistance of cancer [7,8]. Although STAT3 activation is temporary and unnecessary in normal cells, it is dependent on activation of STAT3 to achieve cell survival in many blood

Abbreviations: BCSCs, breast cancer stem cells; bFGF, basic fibroblast growth factor; BSA, Bovine Serum Albumin; DEAB, Diethylamino-benzaldehyde; DMEM, Dulbecco's Modified Eagle's Medium; DMSO, dimethylsulfoxide; DOX, doxorubicin; EMSA, Electrophoretic mobility shift assay; Euc, Eucannabinolide; FBS, fetal bovine serum; hEGF, human epidermal growth factor; Luc, luciferase; STAT3, Signal transducer and activator of transcription 3; TNBC, triple negative breast cancer; Tyr705, tyrosine 705.

* Corresponding authors.
E-mail addresses: ybtcm@zcmu.edu.cn (B. Yang), zhj@zcmu.edu.cn (H. Zhao).

☆ Conflict of interest: The authors declare that there is no conflict of interest.

☆☆ Funding: This work was financially supported by National Natural Science Foundation of China (81774003 and 81773868).

[1] Zhihui Zhu and Jingtao Yuan contributed equally to this article.

Received 22 September 2020; received in revised form 25 October 2020; accepted 27 October 2020

https://doi.org/10.1016/j.neo.2020.10.012

and solid cancers, indicating that targeting abnormal STAT3 activation is a promising therapeutic strategy [9]. Several STAT3 inhibitors have been reported, but they have not been approved by the regulatory authorities. There is an urgent need for new STAT3 inhibitors that can be tested in clinical trials. Recent articles showed that activated STAT3 was found in TNBC. Surprisingly, 80% of TNBC cells expressed activated STAT3 [10,11]. Notably, a significant relationship between constitutive activation of STAT3 and breast cancer stem cell (BCSC)-like properties was observed [11–14]. BCSCs are proved to promote tumor initiation, growth and propagation [15].

Natural products are a well-known treasure house for the development of novel drugs, such as artemisinin, arsenic and paclitaxel [16–18]. Eupatorium cannabinum Linn. is a traditional Chinese medicine in Eupatorium (Compositae) [19]. In previous study, we found that several compounds/active fractions extracted from Eupatorium have anti-tumor activity [20–23]. Eucannabinolide (Euc) is a novel sesquiterpene lactone separated from Eupatorium cannabinum Linn.

In this study, we first found that Euc could suppress the activation of STAT3. We hypothesized Euc as a STAT3 inhibitor and place emphasis on the mechanisms responsible for its novel effects against cell viability, proliferation, metastasis and BCSC-like properties *in vitro* and *in vivo*.

Materials and methods

Cell culture

Human TNBC cell lines MDA-MB-468, MDA-MB-231, and normal mammary epithelial cells, Michigan Cancer Foundation (MCF)-10A were purchased from the Cell Bank of the Institute of Biochemistry and Cell Biology, Chinese Academy of Sciences (Shanghai, China). MDA-MB-231-Luc cells (stably-transfected with luciferase reporter) was a gift from Prof Jian Ding (Shanghai Institute of Material Medical, Shanghai, China). TNBC cells were cultured in DMEM culture medium (Gibco, Gaithersburg, MD, USA) containing 10% fetal bovine serum, (Gibco),100 U/mL penicillin G, 2.5 μg/mL amphotericin B, and 100 μg/mL streptomycin. MCF-10A cells were maintained in DMEM supplemented with hydrocortisone (0.5 μg/mL), insulin (10 μg/mL), endothelial cell growth supplements (20 ng/mL; Sigma, St. Louis, MO, USA), and 10% fetal bovine serum. Cells were incubated at 37 °C with 5% CO_2 in a humidified atmosphere.

Western blotting

Total cell lysates were prepared in radio immunoprecipitation assay (RIPA) lysis buffer containing phenylmethanesulfonyl fluoride (PMSF). Cytosolic and nuclear extracts were obtained using a Nuclear and Cytoplasmic Protein Extraction kit (Beyotime, Shanghai, China) according to the manufacturer's protocols. Equal quantity of proteins was separated on SDS-PAGE gels and transferred onto polyvinylidene difluoride membranes (Millipore, Bedford, MA, USA). The membranes were then blocked with 5% non-fatmilk, incubated with primary antibodies overnight at 4 °C and followed by the appropriate secondary antibodies. The primary antibodies used in the study were as follows: anti-p-STAT3 (Tyr705, #4113, CST, Beverly, MA, USA), anti-p-STAT3 (Ser727, #9134, CST), anti-STAT3 (#9139, CST, USA), anti-Bcl-2 (#2870, CST), anti-MMP-2 (#40994, CST), anti-c-Myc (#9402, CST), anti-EGFR (#4267, CST), anti-p-JAK1 (#3331, CST), anti-JAK1 (#3344, CST), anti-p-ERK (#9101, CST), anti-ERK (#9102, CST), anti-p-STAT1(Tyr701, #9167, CST), anti-STAT1 (#14994, CST), anti-p-STAT5 (Tyr694, #9359, CST), anti-STAT5 (#94250, CST), anti-PARP (#9532, CST), anti-cleaved caspase3 (#9661, CST), anti-caspase3 (#9662, CST), anti-β-actin (#4970, CST), anti-β-tubulin (#2128, CST), anti-survivin (ab76424, abcam, Cambridge, MA, USA), anti-cyclin D1(ab226977, abcam), anti-p-EGFR (Tyr1173, ab32578, abcam), anti-vimentin (ab133260, abcam), anti-ZEB1 (sc-25388, SANTA, Dallas, TX, USA), and anti-H3 (AH433, Beyotime). Horseradish peroxidase (HRP)-conjugated anti-mouse/rabbit IgG (#7076/#7074, CST) was used as the secondary antibody. Immunoblotting signals were detected using the ECL detection system (Bio-Rad, Hercules, CA, USA).

Immunofluorescence

Cells were fixed and permeabilized and incubated with primary antibody. Alexa-conjugated secondary antibodies (Alexa Fluor488 goat anti-rabbit IgG, Jackson Immuno Research, West Grove, PA, USA) were used and incubated. Cell nucleus was then stained with 2-(4-Amidinophenyl)-6-indolecarbamidine dihydrochloride (DAPI). Cells were observed under a fluorescence microscope (Nikon, Tokyo, Japan).

Electrophoretic mobility shift assay

STAT3/DNA-binding activity was detected by electrophoretic mobility shift assay using a Chemiluminescent electrophoretic mobility shift assay Kit (Beyotime) according to the manufacturer's protocols. Nuclear extracts were incubated with double-stranded oligonucleotide probe (STAT3 binding sites 5′-GATCCTTCTGGGAATTCCTAGATC-3′).

Luciferase reporter assay

Cells were co-transfected with STAT3-promoter-Luc and pR-CMV using Lipofectamine 2000 (Invitrogen, Carlsbad, CA, USA). Luciferase activity was assessed by Dual-Glo Luciferase Assay System (Promega, Madison, WI, USA) using a cell Imaging Multi-mode Reader (BioTek, Winooski, VT, USA).

STAT3 knockdown experiments

Short hairpin RNAs (shRNA) was used to package into lentivirus (LV). Approximately 2×10^5 cells were cultured in a six-well plate and transfected with LV-shRNA targeting STAT3. Following transfection, cells were then treated with Euc. Proteins were subsequently isolated and analyzed by western blotting.

Cell viability assay

Cells were seeded in a 96-well cell culture plate. After treatment with Euc, cells were incubated with methylthiazolyldiphenyl-tetrazolium bromide (MTT) solution for 4 h and dissolved in 150 μL dimethylsulfoxide. Cell viability was measured by scanning with a cell Imaging Multi-mode Reader (BioTek) using a 570 nm filter.

Plate colony formation assay

Cells were seeded in a 24-well plate. After treatment with different concentration of Euc, the cells were cultured for another 14 d. The colony formation was observed under a microscope.

Cell apoptosis analysis

Cell apoptosis was detected by Annexin V-FITC/7-AAD dual staining kit (BD Pharmingen, San Diego, CA, USA) and analyzed by Guava Easy Cytometer (Guava Technologies; Merck KGaA, Darmstadt, Germany).

Wound-healing assay

Cells were seeded in a 24-well plate and allowed to form a confluent monolayer. Subsequently, the monolayers were scratched to form perpendicular wounds. The scratched areas were photographed under a microscope and analyzed by Image J software to measure the width of wound.

Boyden chamber migration and invasion assays

6.5-mm chambers with 8-μm pores (Corning, Corning, NY, USA) were used to investigate cell migration and invasion. Cells were plated on the top side of polycarbonate transwell filters (transwell migration assay) or polycarbonate transwell filters coated with 1 μg matrigel (transwell invasion assay) in the upper chambers. Migrated or invaded cells were fixed with methanol and stained with hematoxylin and eosin. Images of five random fields were captured from each membrane with a microscope.

Mammosphere formation assay

Cells were plated in ultra-low-attachment six-well plates (Corning) and cultured in DMEM/F12 serum free medium (Gibco), supplemented with B27 (1:50, Invitrogen), 20 ng/mL basic fibroblast growth factor (bFGF, Sigma), 20 ng/mL human epidermal growth factor (Sigma), 5 μg/m Insulin, 0.4% Bovine Serum Albumin (BSA), at 37 °C in an atmosphere of 5% CO_2. The number and volume of the mammospheres were photographed under an inverted microscope (Nikon).

$CD44^+/CD24^-$ staining

Cells were harvested, stained with fluorescein isothiocyanate (FITC)- and PE-conjugated anti-mouse IgG or FITC-conjugated anti-CD44 and PE conjugated anti-CD24 antibodies (BD Biosciences) and then analyzed by flow cytometry (Guava Technologies).

Aldefluor-positivity assay

An Aldefluor assay kit (Stem cell Technologies, Vancouver, Canada) was used to assess ALDH1 activity. Diethylamino-benzaldehyde was used as a specific inhibitor of ALDH1 to define the Aldefluor-positive population. Cells were analyzed by flow cytometry (Guava Technologies).

In vivo *study*

The animal studies were approved by the Institutional Animal Care and Use Committee of Zhejiang Chinese Medical University (no ZSLL-2013-108) and performed according to the Guidelines proposed by the Laboratory Animal Research Center of Zhejiang Chinese Medical University. For xenograft model, MDA-MB-231 cells were injected subcutaneously into 4-wk-old BALB/c nu/nu female mice (Shanghai Experimental Animal Center, Shanghai, China). Upon tumor volume reaching 50 mm^3, the mice were randomly assigned to vehicle control, positive control (doxorubicin, DOX, 3 mg/kg) and Euc (30 mg/kg). Drugs were administered by intraperitoneal (ip) injection every other day for 26 d. Tumor volume was calculated using the following equation: volume = ($width^2$ × length)/2.

For lung metastasis model, MDA-MB-231-Luc cells (5×10^5 in 0.1 mL DMEM/F12 serum free medium) were intravenously injected subcutaneously into 4-wk-old BALB/c nu/nu female mice through the tail vein. The mice were randomly assigned to vehicle control and Euc (30 mg/kg). Following injection, the mice were treated with Euc (30 mg/kg) or saline for 9 d. The mice were then anesthetized and subjected to an *in vivo* imaging system (Nikon) to image. After sacrifice, lung metastatic tumors were counted.

Immunohistochemistry and tunel staining

Tissues were fixed in 10% formalin and embedded in paraffin. Sections were dewaxed and rehydrated. The primary antibody was used for incubation overnight at 4 °C. The slides were then incubated in HRP horseradish peroxidase, stained with DAB (ZSGB-BIO, Beijing, China), counterstained with hematoxylin. Apoptosis was detected by TUNEL staining kit (Yeasen, Shanghai, China) according to the manufacturer's protocols.

Statistical analysis

All data were analyzed using GraphPad Prism 5.0 statistical software (SanDiego, USA). The results are performed at least three independent experiments and presented as mean ± SEM. Statistical analysis was performed using a two tailed Student's *t* test. The criterion of statistical significance was $^*P< 0.05$; $^{**}P< 0.01$; $^{***}P< 0.001$.

Results

Euc suppressed constitutive and interleukin-6-induced STAT3 activation

In previous study, we found that sesquiterpene lactones of Eupatorium lindleyanumhas notable inhibition of STAT3 activity and a potential cytotoxic activity against TNBC cells [23]. We hypothesized that there may be a compound of sesquiterpene lactone in Eupatorium that plays anti-tumor role via highly inhibiting STAT3 activity. To clarify the hypothesis, we first found Eucannabinolide (Euc) (Figure 1a), a sesquiterpene lactones, could inhibited constitutive STAT3 phosphorylation at tyrosine705 (Tyr705) in TNBC cells. The inhibition has been evident since 15 min. However, treatment of Euc did not affect STAT3 phosphorylation at serine727 and the expression total STAT3 (Figure 1b). The phosphorylation of STAT3 usually occurs at Tyr705, followed by dimerization, nuclear translocation and binding to consensus promoter sequence of their target genes to initiate transcription [24]. Thus, the nuclear translocation of p-STAT3 (Tyr705) was explored. As shown in Figure 1c, the expression of p-STAT3 (Tyr705) in nuclear was decreased after Euc treatment, the fluorescence also attenuated (Figure 1d). Furthermore, we found that Euc led to inhibition of STAT3 DNA-binding activity in a dose-dependent in the two TNBC cells (Figure 1e). However, when a luciferase reporter assay was used to identify transcription activation of STAT3, we found that Euc did not affect STAT3 transcription itself (Figure 1f), indicating Euc works by inhibiting p-STAT3 (Tyr705) rather than STAT3 protein expression itself.

STAT3 is initially activated by tyrosine phosphorylation in response to interleukin-6 (IL-6) [25]. In TNBC subtype, autocrine and paracrine production of the IL-6 family of cytokines constitute the major mechanism of STAT3 activation. The effect of Euc on IL-6-stimulated STAT3 phosphorylation was examined. Our results showed that p-STAT3 (Tyr705) was successfully stimulated after treatment of IL-6 and Euc inhibited IL-6-induced STAT3 phosphorylation (Figure 1g). The above results demonstrated that Euc could inhibit the activity of STAT3 via autocrine and paracrine production of the IL-6.

Euc was considered as a STAT3 inhibitor

Tyrosine residues on STAT3 protein are phosphorylated by various upstream signaling cascades, including JAKs, Src, EGFR and MAPKs. To determine whether the inhibitory effect of Euc on STAT3 phosphorylation

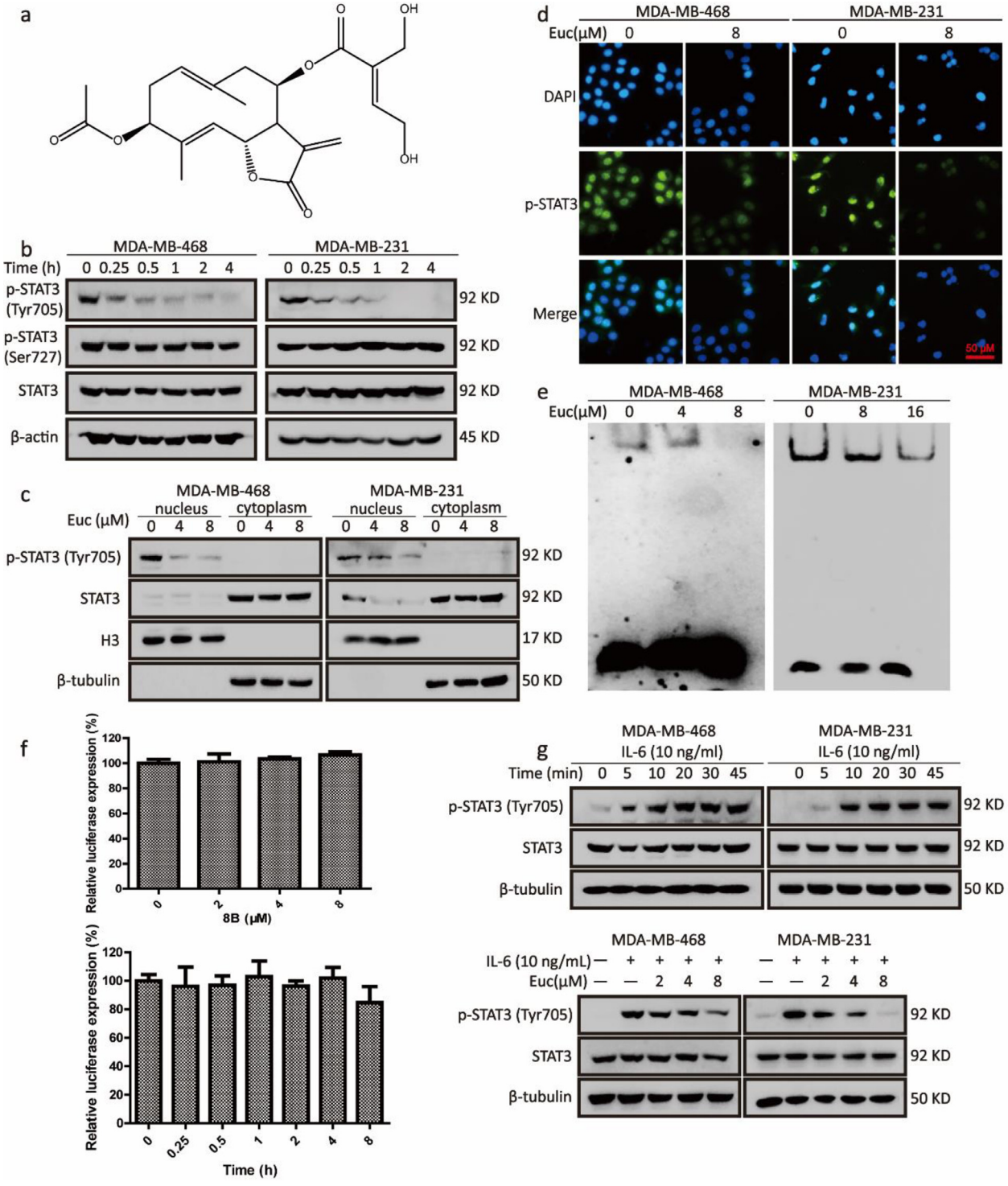

Figure 1. Euc inhibited the constitutive and IL-6-induced STAT3 activation. (a) The chemical structure of Euc. (b) Western blotting analysis of STAT3 phosphorylation at Tyr705 and Ser727 expression levels after treated with Euc at the indicated times. (c) Western blotting and (d) immunofluorescence analysis of STAT3 nuclear translocation after treated with Euc. (e) Effect of Euc on the DNA-binding activity of STAT3 was detected by EMSA assay. (f) Effect of Euc on transcription activation of STAT3 was detected by a luciferase reporter assay. (g) Cells were treated with IL-6 (10 ng/mL) for different times (upper). Cells were stimulated with IL-6 (10 ng/mL) for 10 min and treated with Euc for another 4 h (under). The activity of STAT3 was detected by western blotting.

is due to the suppression of upstream signaling pathways, we evaluated the effect of Euc on the activation of JAK, EGFR and ERK. Our results showed that Euc slightly reduced the expression of p-JAK1, JAK1 and has little effect on EGFR, p-ERK, ERK. However, the expression of p-STAT3 (Tyr705) was almost completely inhibited (Figure 2a), indicating that Euc may directly inhibit STAT3 activity rather than affecting the upstream signal pathway. Since Euc could inhibit the activity of STAT3, the downstream target genes of STAT3 were then tested. After Euc treated, the expression of Bcl-2, survivin, MMP-2, cyclin D1, c-Myc was inhibited (Figure 2b). To investigate whether Euc selectively suppresses p-STAT3, the activity of other STATs family proteins was examined. We found that Euc had little inhibitory effect on p-STAT1, STAT1, p-STAT5 and STAT5. The expression of p-STAT3 (Tyr705) was almost completely inhibited (Figure 2a), suggesting that Euc inhibits STAT3 activation selectively as well as considered as a STAT3 inhibitor.

Inhibition of p-STAT3 (Tyr705) or knockdown of STAT3 attenuated the inhibitory effect on Euc-induced cell viability

Based on the above results, we assumed that Euc might target STAT3 to inhibit the viability of TNBC cells. To confirm this, STAT3 siRNA and STAT3 inhibitor were introduced to block STAT3 and p-STAT3 (Tyr705), respectively. As shown in Figure 2c, STAT3 was successfully inhibited after lentivirus transfection of STAT3-shRNA. Then the cells of negative control (NC), shRNA-1 and shRNA-2 were treated with Euc and cell viability was detected. The results showed that the relative cell viability of NC was more decreased than that of shRNA-1 and shRNA-2 (Figure 2d). To further confirm this result, S3I-201 as a STAT3 inhibitor was used to inhibit STAT3 phosphorylation at Tyr705 (Figure 2c). The TNBC cells were pre-treated with or without S3I-201 for 2 h and then treated with Euc for another 24 h. The relative cell viability of Euc treatment alone was more decreased than that of Euc combined with S3I-201 (Figure 2d). The above data indicated that Euc could inhibit TNBC cells via targeting STAT3.

Euc inhibited cell growth via inducing cell apoptosis in a caspase-dependent manner

Our above data demonstrate that Euc can block the activation of STAT3 directly, selectively, and effectively. Inhibition of STAT3 are closely related with tumor growth and metastasis. Therefore, we investigated whether Euc could suppress cell growth and metastasis in TNBC cells. To determine the effects of Euc on cell growth, human TNBC cell lines and human mammary epithelial MCF-10A cells were involved. In TNBC cells, Euc exhibited significantly growth-inhibitory activities in a dose- and time-dependent manner (Figure 3a). At the same concentration, cell viability of MCF-10A was almost no inhibited after Euc treatment for 48 h (Figure 3b). In plate colony formation assay, two TNBC cells were cultured and treated with Euc. The colony number and size were reduced in Euc treatment cells (Figure 3c). The results indicated that Euc inhibited cell proliferation.

To further investigate whether Euc-induced cell death was associated with apoptotic cell death, Annexin V-FITC/7AAD staining was used. Euc could elicited apoptosis in a dose-dependent manner (Figure 4a). And, Euc downregulated protein levels of caspases3 and PARP, upregulated cleaved caspase3 and cleaved PARP (Figure 4c). When pretreated with Z-VAD-FMK, Euc-induced apoptosis was attenuated (Figure 4b), indicating that Euc-induced apoptosis in a caspase-dependent manner. Under the same condition, Euc-induced apoptosis in TNBC cells did not appear in MCF-10A cells (Figure 4d). We detected the expression of STAT3 phosphorylation at Tyr705 after Euc treatment in MCF-10A cells. Consistent with our assumption, there was almost no change in p-STAT3 expression after intervening Euc (Figure 4e). These results suggested that Euc could induce apoptosis through caspase dependent pathway in TNBC without the apoptosis of normal mammary epithelial cells.

Euc inhibited the migration and invasion of TNBC cells

Then we investigated whether Euc suppressed the migration and invasion in TNBC. MTT assay was first performed to detect the cytotoxicity on MDA-MB-231 cells after Euc treatment for 24 h. As shown in Figure 5a, Euc under the concentration of 2 μM showed no cytotoxicity ($P > 0.05$). The concentration of 0.5, 1, 2 μM was selected for the following experiments. Wound-healing assay was performed to detect the effect of Euc on cell migration. Our results showed that the wound closure rate was decreased after Euc treatment for 24 h (Figure 5b). In addition, the migrated cells after Euc treatment for 12 h were less than control in a Boyden chamber migration assay (Figure 5c). Moreover, the result of Boyden chamber invasion assay showed a decrease of cell invasion after Euc treatment for 12 h (Figure 5c). The effect of STAT3 on cell migration and invasion is linked to the upregulated expression of MMPs, ZEB1 and Vimentin [26, 27]. Vimentin is an intermediate filament protein that functions during cell migration to maintain structure and motility [28]. ZEB1 is a transcriptional regulator conferred tumor-initiating and metastatic activities by inducing epithelial-mesenchymal transition [29]. The expression of vimentin and ZEB1 was examined in this study. Our results showed that Euc could inhibit vimentin and ZEB1expression in MDA-MB-231 cells (Figure 5d). These results indicated that Euc could inhibit migration and invasion through vimentin and ZEB1 related pathway.

Euc targeted BCSC-like properties in TNBC cells through inhibiting constitutively active STAT3

STAT3 pathway was preferentially active in $CD44^+CD24^-$ stem cell-like breast cancer cells [11,30]. We hypothesized that Euc might regulate BCSC-like properties in TNBC cells via inhibiting STAT3. Mammosphere-forming ability *in vitro* was first assessed. After Euc treatment for 24 h, a marked decrease in the number and volume of mammospheres derived from MDA-MB-231 and MDA-MB-468 cells was observed (Figure 6a). We then examined the stem cell surface markers $CD44^+/CD24^-$ and the progenitor marker aldehyde dehydrogenase1 (ALDH1). The results showed that Euc reduced the $CD44^+/CD24^-$ stem-like populations and ALDH1 activity (Figure 6b, 6c). It was reported that STAT3 was preferentially active in $CD44^+CD24^-$ stem cell-like breast cancer cells [11]. The expression of p-STAT3 (Tyr705) was detected in adherent and BCSC-like TNBC cells. An increased expression of p-STAT3 (Tyr705) was observed in BCSC-like cells compared with adherent cells (Figure 6d). And, Euc inhibited the expression of p-STAT3 (Tyr705) in BCSC-like cells (Figure 6d), suggested that Euc targeted BCSC-like properties in TNBC cells through inhibiting constitutively active STAT3.

Euc suppressed tumor growth and lung metastasis via inactivation of STAT3 signaling in vivo

Given its encouraging *in vitro* findings of Euc on cell proliferation, migration and invasion, we further investigated the *in vivo* effect on tumor mass. MDA-MB-231cells were injected subcutaneously into BALB/c female mice to establish a xenograft model. As shown in Figure 7a and b, the tumor volume was significantly decreased in Euc-or DOX-treated group. Tumor weight inhibition was evident in mice that adopted Euc or DOX compared with the control (Figure 7c). Additionally, there was no difference of body weight between Euc and control groups, meaning that Euc might be considered to be relatively safe without obvious toxicity. While, an obvious toxicity in DOX group was found ($P< 0.001$, Figure 7d).

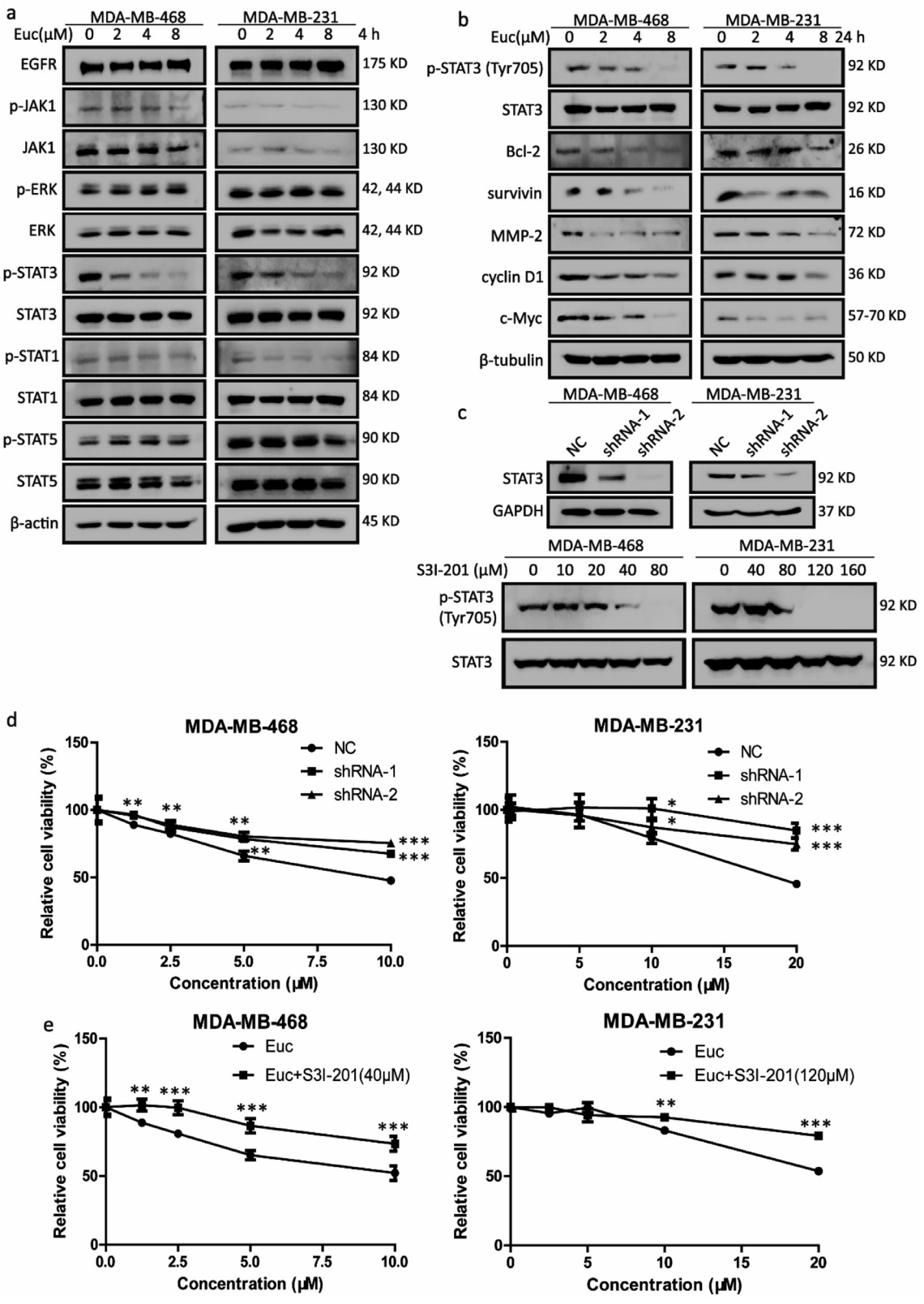

Figure 2. Euc acted as a STAT3 inhibitor. (a) The expression of upstream target genes of STAT3 and STATs family proteins was detected by western blotting after treatment of Euc for 4 h. (b) The expression of downstream target genes of STAT3 was detected by western blotting after treatment of Euc for 24 h. (c) The expression of STAT3 after transfection of STAT3-shRNA (upper) or incubation with S3I-201 (under) were detected by western blotting. (d) The viability of TNBC cells treated with Euc was detected by MTT assay after transfection of STAT3-shRNA cells or incubation with S3I-201.

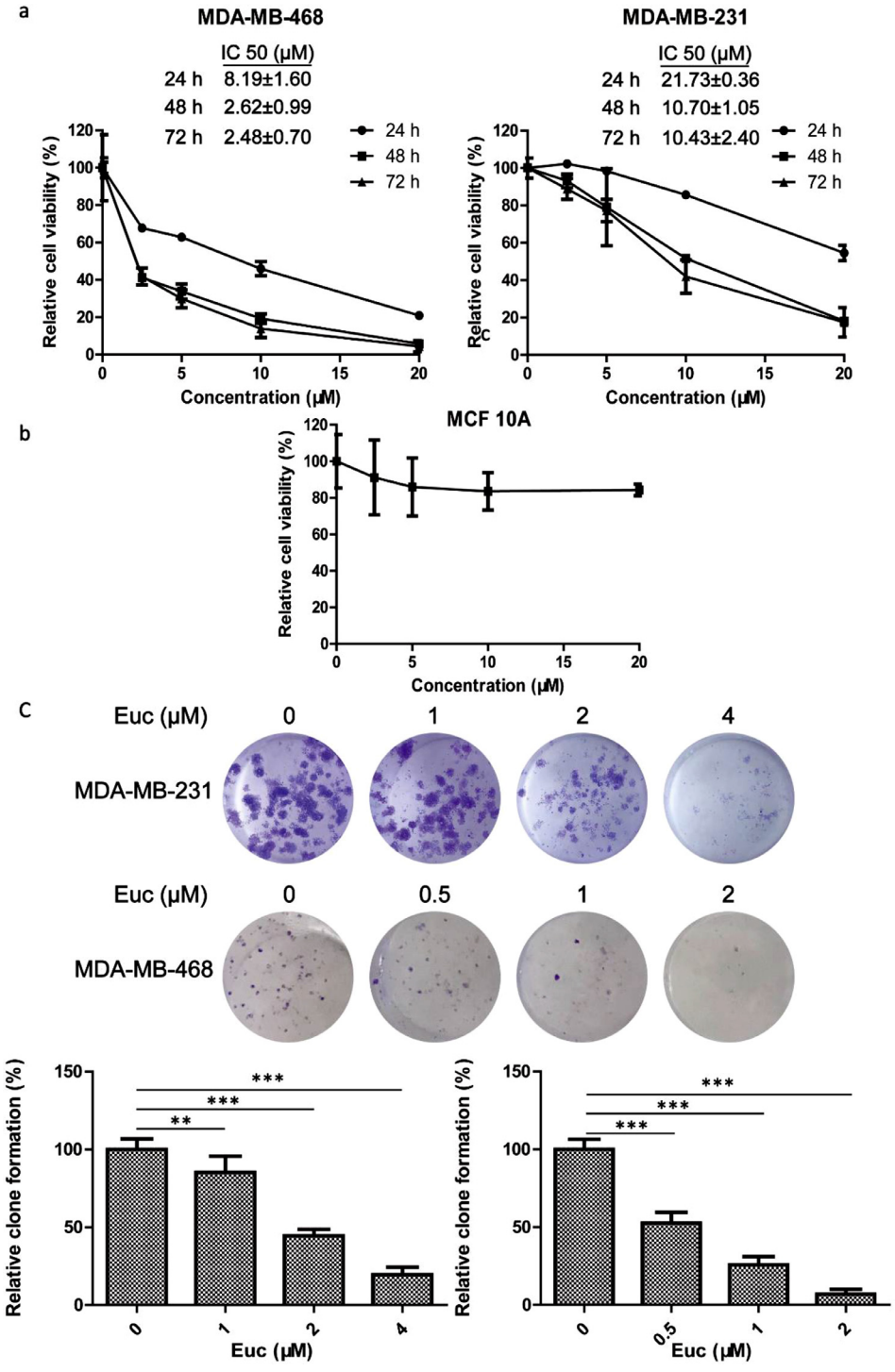

Figure 3. Euc inhibited the growth of TNBC cells. (a) Effects of Euc on the viability of TNBC cells were detected MTT assay. (b) The viability of MCF-10A cells was quantified by the MTT assay after treatment with Euc for 48 h. (c) Cell proliferation was measured by plate colony formation assay after treatment with Euc for 14 d (upper) and quantified (under).

Apoptosis was assessed by TUNEL. As shown in Figure 7e, the number of TUNEL-positive cells increased in the tumor tissues of Euc-treated mice. We additionally detected whether Euc-mediated suppression of tumor growth were accompanied by the inhibition of STAT3 activation. Immunohistochemical analysis demonstrated that Euc resulted in a decrease in p-STAT3, MMP-2, and survivin (Figure 7f). These data suggested that Euc could suppress tumor growth and via inactivation of STAT3 signaling.

To further evaluate the anti-metastatic effects of Euc *in vivo*, a lung metastasis model was used. After the mice treated with Euc or saline for 9 d, an obvious decrease of cancer metastasis was observed in the lungs in of Euc-

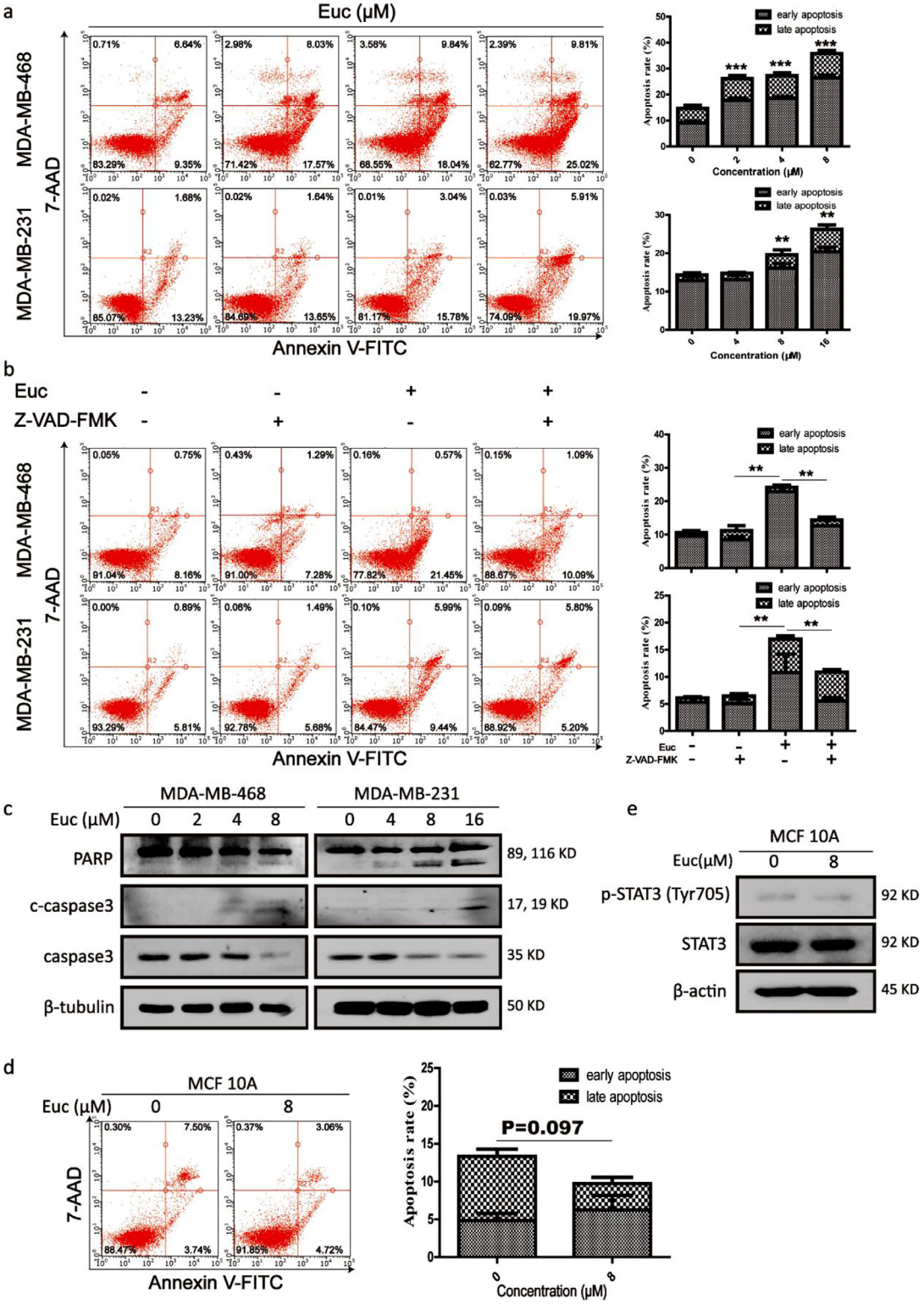

Figure 4. Euc induced apoptosis in TNBC cells. (a) The apoptotic cells were stained with Annexin V-FITC/7AAD and analyzed by flow cytometry. (b) Cells were treated with Euc for 24 h after pre-treatment with caspase inhibitor Z-VAD-FMK (20 μM) for 2 h. Cell apoptosis was analyzed by flow cytometry. (c) Western blotting analysis was preformed to detect the expression of caspase relative proteins. (d) Apoptosis of MCF-10A cells after treatment with Euc was detected by flow cytometry. (e) The expression of p-STAT3 (Tyr705) after treatment with Euc for 24 h in MCF-10A cells was detected by western blotting.

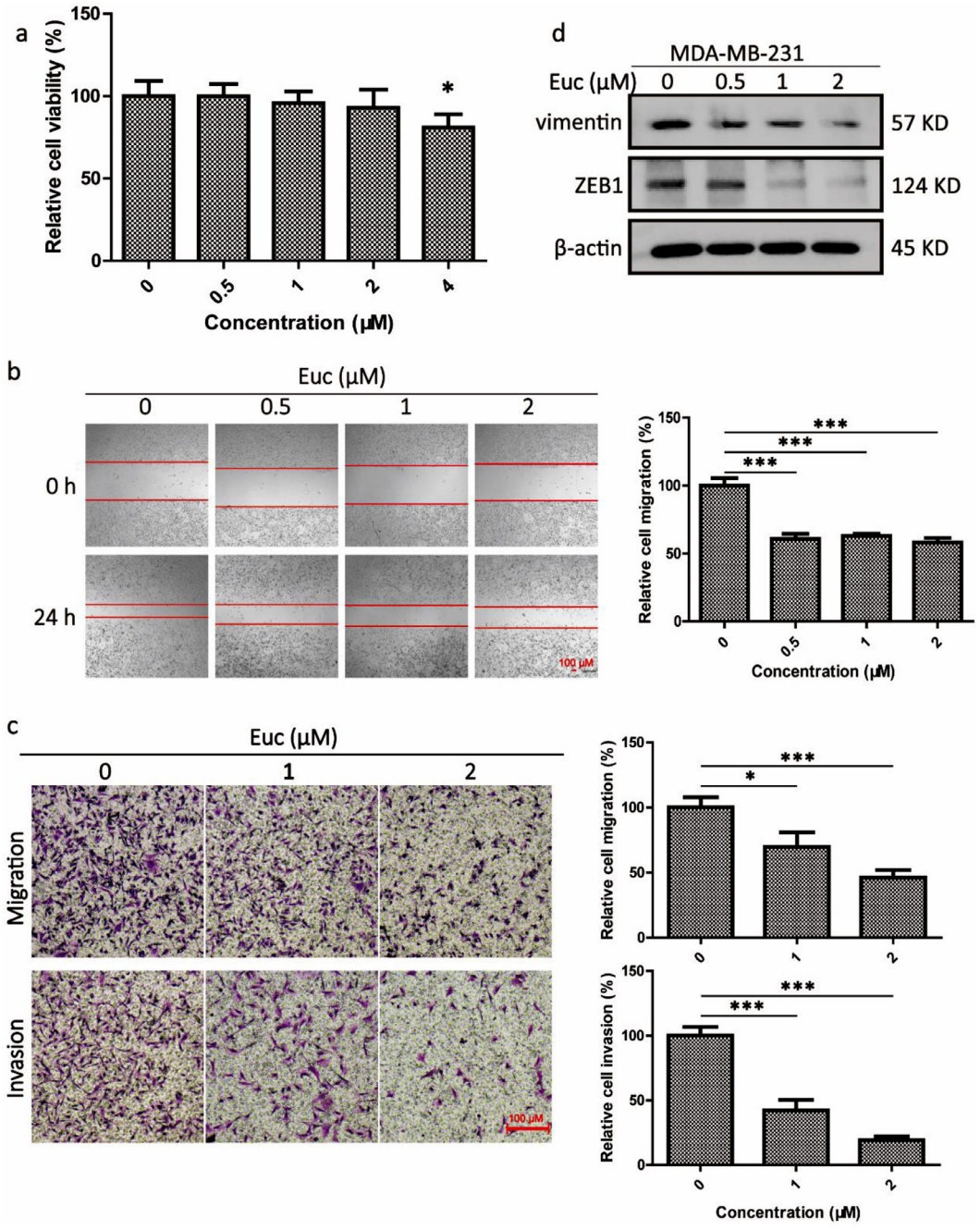

Figure 5. Euc inhibited the migration and invasion of MDA-MB-231 cells. (a) The non-cytotoxicity dose of Euc on MDA-MB-231 cells was assayed by MTT. (b) Cell monolayers were scratched and the cells were exposed to Euc for 24 h. The migratory cells were observed under a microscope. (c) Cells were seeded onto transwell chambers (upper) or matrigel-coated transwell chambers (under) and incubated with Euc for 24 h. The migrated or invaded cells were observed under a microscope. (d) The expression of vimentin and ZEB1 was detected by western blotting.

treated group (Figure 7g). The lung metastatic nodules were reduced in Euc-treated group (Figure 7h). In addition, there was no observed sign of toxicity, as judged by parallel monitoring of body weight ($P > 0.05$, Figure 7i). These data demonstrated that Euc was a relatively safe compound and inhibited TNBC metastasis *in vivo*.

Discussion

In the present study, we showed that Eucannabinolide suppressed the proliferation, metastasis and BCSC-like traits in TNBC via targeting STAT3. We demonstrated for the first time that Euc can suppress constitutive and IL-6-induced STAT3 activation in TNBC cells via selectively inhibiting STAT3 phosphorylation at Tyr705, resulting in the suppression of STAT3 nuclear translocation and DNA-binding activities to inhibit the expression of its downstream target genes. Thus, Euc may be developed as a STAT3 inhibitor or potential therapeutic for TNBC.

Abundant evidence has demonstrated that STAT3 may be a promising drug target for TNBC therapy. In TNBC, STAT3 is overexpressed and constitutively activated, associated with poor survival outcomes. Recent research reported that STAT3 was persistently phosphorylated in basal breast

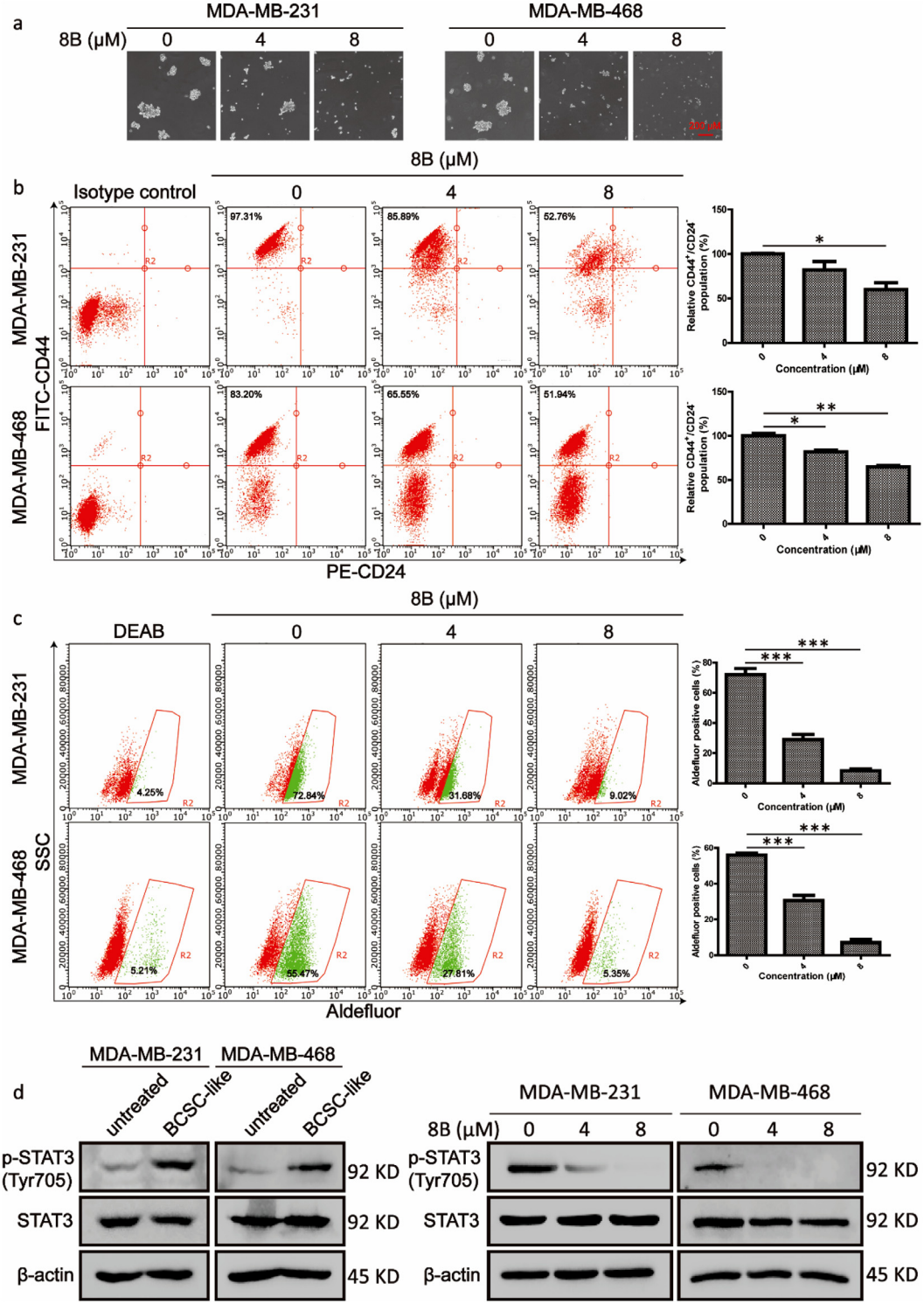

Figure 6. Euc suppressed BCSC-like properties in TNBC cells. (a) MDA-MB-231 and MDA-MB-468 were cultured in serum-free suspension conditions. The number and volume of mammospheres after treated with Euc was quantified by optical microscope. The mammospheres of $CD44^{+}/CD24^{-}$ populations (b) and ALDH1 activity (c) after treated with Euc were evaluated by flow cytometry. (d) The expression of p-STAT3 (Tyr705) between adherent and BCSC-like cells (left) or after treatment with Euc in BCSC-like cells (right) was detected by western blotting.

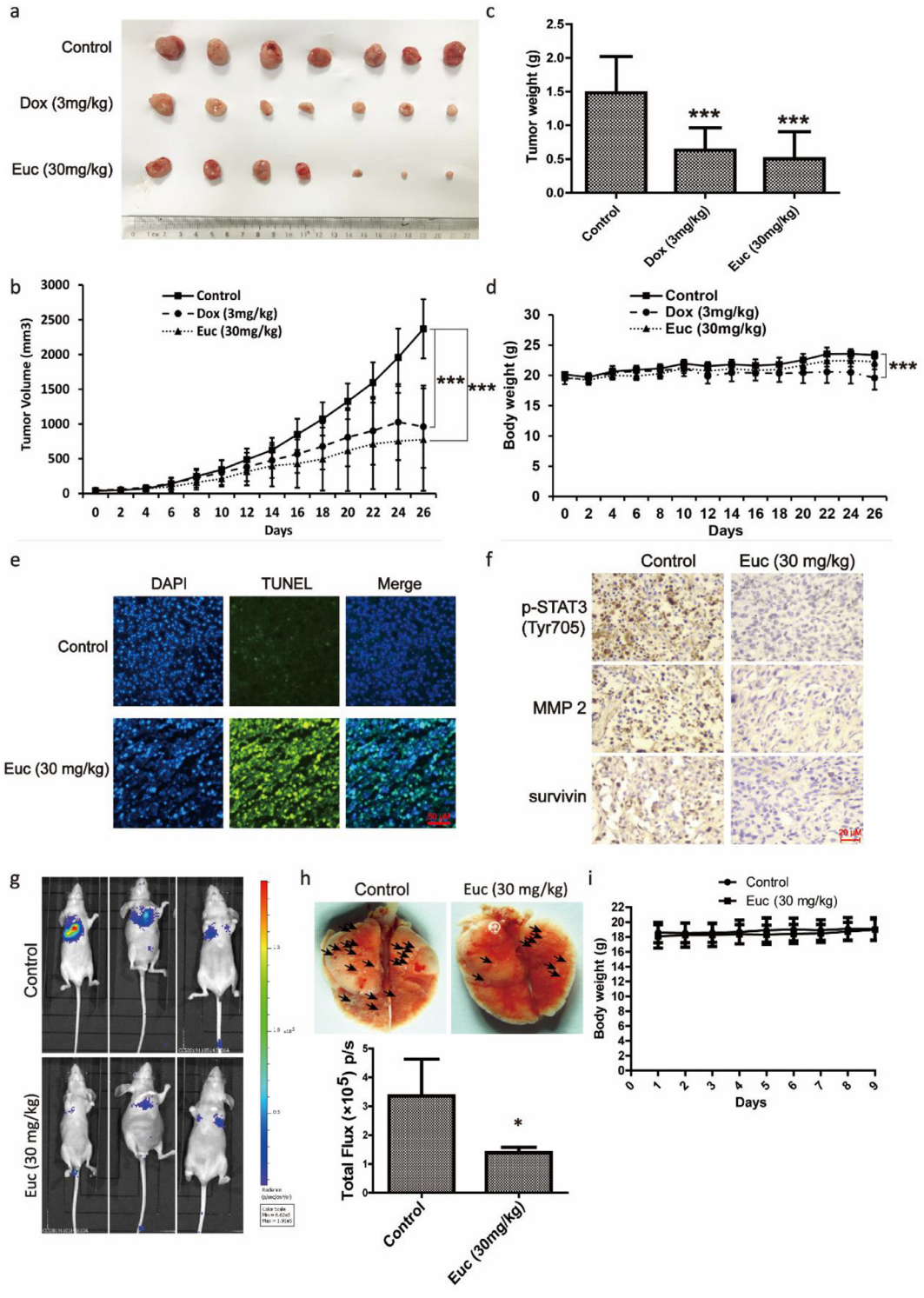

Figure 7. Euc inhibited the growth and metastasis of TNBC *in vivo*. (a) After treatment with Euc for 26 d, representative tumor images were photographed. (b) Tumor sizes were recorded every other day by vernier caliper measurements and calculated. (c) And tumor masses were weighted. (d) The average body weight of mice with xenografts was consecutively recorded. (e) Tumor apoptosis was detected by TUNEL staining. (f) The expression of p-STAT3, MMP-2 and survivin was detected by immunohistochemistry. (g) Bioluminescence imaging of nude mice lung metastasis model were photographed after treatment with Euc for 9 d. (h) The lung metastatic nodules were photographed. (i) The average body weight of mice was consecutively recorded.

cancer cells and in low levels in luminal breast cancer cells [10,31]. STAT3 activation is associated with cancer cell proliferation, survival, metastasis, and chemo-resistance [32,33]. Inhibitors of STAT3 have potential uses in the treatment and prevention of cancer [34]. STAT3 is initially activated by tyrosine phosphorylation in response to IL-6 [25]. Thus, the constitutive or induced STAT3 activation was first detected in this study. And we demonstrate that Euc can suppress both constitutive and IL-6-induced STAT3 activation and the processes of p-STAT3 dimerization, nuclear translocation and DNA binding activities were subsequently attenuated.

Accumulating studies have shown that STAT3 is highly represented for growth of $CD44^+CD24^-$ stem cell-like breast cancer cells, especially in basal-like breast cancer and maintains the self-renewal differentiation of cancer stem cells [11]. Inhibition of STAT3 impairs CSC-like traits, leading to suppression of tumor development. In this study, we demonstrated that STAT3 phosphorylation at Tyr705 is predominantly elevated in BCSC-like populations of TNBC cells. Administration of Euc impaired mammosphere formation, reduced the $CD44^+CD24^-$ subpopulation and inhibited ALDH1 activity of stem cell-like properties, followed with reducing the expression of p-STAT3 (Tyr705), indicating that Euc-reduced stem cell-like properties may be attributable to the suppression of STAT3 signaling.

The important goal of cancer drug discovery is to develop therapeutic agents that are effective, safe, and affordable. In our study, Euc has a potential therapeutic window with IC50 of below 10 μM for TNBC cells and almost non-toxicity for mammary epithelial cells in the same condition. What's more, Euc inhibited the growth and metastasis of TNBC *in vivo*, but did not affect the weight of nude mice, suggested that 30 mg/kg Euc might not cause sever adverse effect. However, developing Euc into cancer therapeutics needs to be cautiously warrant in future development for TNBC.

In conclusion, we identified Euc elicits anti-tumor effects in TNBC via targeting STAT3. Euc may be developed as anti-cancer drugs by targeting STAT3 phosphorylation at Tyr705 and inhibiting the STAT3 signaling pathway.

Author contributions

Huajun Zhao: Conceptualization, Data Curation, Formal analysis, Investigation, Methodology, Project administration, Validation and Visualization. Bo Yang: Project administration, Extracted and identified Euc. Zhihui Zhu: Data Curation, Formal analysis, Investigation, Methodology, Writing-original draft, Writing-review & editing. Jingtao Yuan: Investigation, Formal analysis. Xintong Xu: Investigation, Data Curation. Yingying Wei: Investigation, Data Curation.

References

[1] DeSantis CE, Ma J, Gaudet MM, Newman LA, Miller KD, Goding Sauer A, Jemal A, Siegel RL. Breast cancer statistics. *2019 CA Cancer J Clin* 2019;**69**:438–51.

[2] Diamond JR, Eckhardt SG, Pitts TM, van Bokhoven A, Aisner D, Gustafson DL, Capasso A, Sams S, Kabos P, Zolman K, et al. A phase II clinical trial of the Aurora and angiogenic kinase inhibitor ENMD-2076 for previously treated, advanced, or metastatic triple-negative breast cancer. *Breast Cancer Res BCR* 2018;**20**:82.

[3] Varghese S, Samuel SM, Varghese E, Kubatka P, Busselberg D. High glucose represses the anti-proliferative and pro-apoptotic effect of metformin in triple negative breast cancer cells. *Biomolecules* 2019;**9**:1–16.

[4] Robert M, Patsouris A, Frenel JS, Gourmelon C, Augereau P, Campone M. Emerging PARP inhibitors for treating breast cancer. *Expert Opin Emerg Drugs* 2018;**23**:211–21.

[5] Costa R, Shah AN, Santa-Maria CA, Cruz MR, Mahalingam D, Carneiro BA, Chae YK, Cristofanilli M, Gradishar WJ, Giles FJ. Targeting Epidermal Growth Factor Receptor in triple negative breast cancer: new discoveries and practical insights for drug development. *Cancer Treat Rev* 2017;**53**:111–19.

[6] Brown C. Targeted therapy: an elusive cancer target. *Nature* 2016;**537**:S106–8.

[7] Abubaker K, Luwor RB, Escalona R, McNally O, Quinn MA, Thompson EW, Findlay JK, Ahmed N. Targeted disruption of the JAK2/STAT3 pathway in combination with systemic administration of paclitaxel inhibits the priming of ovarian cancer stem cells leading to a reduced tumor burden. *Front Oncol* 2014;**4**:75.

[8] Chun J, Li RJ, Cheng MS, Kim YS. Alantolactone selectively suppresses STAT3 activation and exhibits potent anticancer activity in MDA-MB-231 cells. *Cancer Lett.* 2015;**357**:393–403.

[9] Xiang M, Kim H, Ho VT, Walker SR, Bar-Natan M, Anahtar M, Liu S, Toniolo PA, Kroll Y, Jones N, et al. Gene expression-based discovery of atovaquone as a STAT3 inhibitor and anticancer agent. *Blood* 2016;**128**:1845–53.

[10] Chang R, Song L, Xu Y, Wu Y, Dai C, Wang X, Sun X, Hou Y, Li W, Zhan X, et al. Loss of Wwox drives metastasis in triple-negative breast cancer by JAK2/STAT3 axis. *Nat Commun* 2018;**9**:3486.

[11] Marotta LL, Almendro V, Marusyk A, Shipitsin M, Schemme J, Walker SR, Bloushtain-Qimron N, Kim JJ, Choudhury SA, Maruyama R, et al. The JAK2/STAT3 signaling pathway is required for growth of CD44(+)CD24(-) stem cell-like breast cancer cells in human tumors. *J Clin Invest* 2011;**121**:2723–35.

[12] Oh E, Kim YJ, An H, Sung D, Cho TM, Farrand L, Jang S, Seo JH, Kim JY. Flubendazole elicits anti-metastatic effects in triple-negative breast cancer via STAT3 inhibition. *Int J Cancer* 2018;**143**:1978–93.

[13] Kim YJ, Sung D, Oh E, Cho Y, Cho TM, Farrand L, Seo JH, Kim JY. Flubendazole overcomes trastuzumab resistance by targeting cancer stem-like properties and HER2 signaling in HER2-positive breast cancer. *Cancer Lett* 2018;**412**:118–30.

[14] Wei W, Tweardy DJ, Zhang M, Zhang X, Landua J, Petrovic I, Bu W, Roarty K, Hilsenbeck SG, Rosen JM, et al. STAT3 signaling is activated preferentially in tumor-initiating cells in claudin-low models of human breast cancer. *Stem Cells* 2014;**32**:2571–82.

[15] Al-Ejeh F, Smart CE, Morrison BJ, Chenevix-Trench G, Lopez JA, Lakhani SR, Brown MP, Khanna KK. Breast cancer stem cells: treatment resistance and therapeutic opportunities. *Carcinogenesis* 2011;**32**:650–8.

[16] Wang J, Zhang CJ, Chia WN, Loh CC, Li Z, Lee YM, He Y, Yuan LX, Lim TK, Liu M, et al. Haem-activated promiscuous targeting of artemisinin in Plasmodium falciparum. *Nat Commun* 2015;**6**:10111.

[17] Zhu HH, Hu J, Lo-Coco F, Jin J. The simpler, the better: oral arsenic for acute promyelocytic leukemia. *Blood* 2019;**134**:597–605.

[18] Mazieres J, Kowalski D, Luft A, Vicente D, Tafreshi A, Gumus M, Laktionov K, Hermes B, Cicin I, Rodriguez-Cid J, et al. Health-related quality of life with carboplatin-paclitaxel or nab-paclitaxel with or without pembrolizumab in patients with metastatic squamous non-small-cell lung cancer. *J Clin Oncol* 2020;**38**:271–80 JCO1901348.

[19] Wang F, Zhong H, Fang S, Zheng Y, Li C, Peng G, Shen X. Potential anti-inflammatory sesquiterpene lactones from eupatorium lindleyanum. *Planta Med.* 2018;**84**:123–8.

[20] Yang B, Zhao Y, Lou C, Zhao H. Eupalinolide O, a novel sesquiterpene lactone from Eupatorium lindleyanum DC., induces cell cycle arrest and apoptosis in human MDA-MB-468 breast cancer cells. *Oncol Rep* 2016;**36**:2807–13.

[21] Tian S, Chen Y, Yang B, Lou C, Zhu R, Zhao Y, Zhao H. F1012-2 inhibits the growth of triple negative breast cancer through induction of cell cycle arrest, apoptosis, and autophagy. *Phytother Res PTR* 2018;**32**:908–22.

[22] Lou C, Chen Y, Zhang J, Yang B, Zhao H. Eupalinolide J suppresses the growth of triple-negative breast cancer cells via targeting STAT3 signaling pathway. *Front Pharmacol* 2019;**10**:1071.

[23] Yang B, Shen JW, Zhou DH, Zhao YP, Wang WQ, Zhu Y, Zhao HJ. Precise discovery of a STAT3 inhibitor from Eupatorium lindleyanum and evaluation of its activity of anti-triple-negative breast cancer. *Nat Prod Res* 2019;**33**:477–85.

[24] Banerjee K, Resat H. Constitutive activation of STAT3 in breast cancer cells: a review. *Int J Cancer* 2016;**138**:2570–8.

[25] Zhong Z, Wen Z, Darnell JE Jr. Stat3: a STAT family member activated by tyrosine phosphorylation in response to epidermal growth factor and interleukin-6. *Science* 1994;**264**:95–8.

[26] Davis FM, Azimi I, Faville RA, Peters AA, Jalink K, Putney JW Jr, Goodhill GJ, Thompson EW, Roberts-Thomson SJ, Monteith GR. Induction of epithelial-mesenchymal transition (EMT) in breast cancer cells is calcium signal dependent. *Oncogene* 2014;**33**:2307–16.

[27] Ma JH, Qi J, Lin SQ, Zhang CY, Liu FY, Xie WD, Li X. STAT3 targets ERR-alpha to promote epithelial-mesenchymal transition, migration, and invasion in triple-negative breast cancer cells. *Molecul Cancer Res MCR* 2019;**17**:2184–95.

[28] Richardson AM, Havel LS, Koyen AE, Konen JM, Shupe J, WGt Wiles, Martin WD, Grossniklaus HE, Sica G, Gilbert-Ross M, et al. Vimentin is required for lung adenocarcinoma metastasis via heterotypic tumor cell-cancer-associated fibroblast interactions during collective invasion. *Clin Cancer Res* 2018;**24**:420–32.

[29] Tan X, Banerjee P, Liu X, Yu J, Gibbons DL, Wu P, Scott KL, Diao L, Zheng X, Wang J, et al. The epithelial-to-mesenchymal transition activator ZEB1 initiates a prometastatic competing endogenous RNA network. *J Clin Invest* 2018;**128**:3198.

[30] Ibrahim SA, Gadalla R, El-Ghonaimy EA, Samir O, Mohamed HT, Hassan H, Greve B, El-Shinawi M, Mohamed MM, Gotte M. Syndecan-1 is a novel molecular marker for triple negative inflammatory breast cancer and modulates the cancer stem cell phenotype via the IL-6/STAT3, Notch and EGFR signaling pathways. *Mol Cancer* 2017;**16**:57.

[31] Huynh J, Etemadi N, Hollande F, Ernst M, Buchert M. The JAK/STAT3 axis: a comprehensive drug target for solid malignancies. *Semin Cancer Biol* 2017;**45**:13–22.

[32] Egusquiaguirre SP, Liu S, Tosic I, Jiang K, Walker SR, Nicolais M, Saw TY, Xiang M, Bartel K, Nelson EA, et al. CDK5RAP3 is a co-factor for the oncogenic transcription factor STAT3. *Neoplasia* 2020;**22**:47–59.

[33] Park GB, Kim D. MicroRNA-503-5p inhibits the CD97-mediated JAK2/STAT3 pathway in metastatic or paclitaxel-resistant ovarian cancer cells. *Neoplasia* 2019;**21**:206–15.

[34] Bai L, Zhou H, Xu R, Zhao Y, Chinnaswamy K, McEachern D, Chen J, Yang CY, Liu Z, Wang M, et al. A potent and selective small-molecule degrader of stat3 achieves complete tumor regression in vivo. *Cancer Cell* 2019;**36**:498–511 e417.